Supplementary Material

Streamwise dispersion of soluble matter in solvent flowing through a tube

Mingyang Guan[1] and Guoqian Chen[1,2]†

[1]Laboratory of Systems Ecology and Sustainability Science, College of Engineering, Peking University, Beijing 100871, China

[2]Macao Environmental Research Institute, Macau University of Science and Technology, Macao 999078, PR China

(In the format provided by the authors and unedited)

1. Monte–Carlo simulations in the cylindrical coordinate

With a standard Monte–Carlo simulation shown below, we have reproduced the key hallmarks of the four dispersion regimes predicted by the streamwise dispersion theory, as presented in figure 6 in the main text. The numerical scheme is slightly different from that adopted by Houseworth (1984), who simulated the transport of particles by an exact analytical solution in the radial direction and let it walk randomly in the longitudinal direction. With the assumption of isotropic diffusion, the following stochastic differential equations (SDEs) and the convection-diffusion equation (CDE) in the Cartesian coordinates (x_1, y_1, z_1) are considered as equivalent to describe the dispersion process

$$\mathrm{d}x_1 = Pe u\left(y_1, z_1\right) \mathrm{d}t + \sqrt{2}\mathrm{d}w_1, \quad \mathrm{d}y_1 = \sqrt{2}\mathrm{d}w_2, \quad \mathrm{d}z_1 = \sqrt{2}\mathrm{d}w_3$$

$$\Leftrightarrow \frac{\partial P}{\partial t} + Pe u\left(y_1, z_1\right) \frac{\partial P}{\partial x_1} = \left(\frac{\partial^2 P}{\partial {x_1}^2} + \frac{\partial^2 P}{\partial y_1^2} + \frac{\partial^2 P}{\partial z_1^2}\right). \tag{1.1}$$

In the cylindrical coordinates (ξ, r, θ), the corresponding CDE reads

$$\frac{\partial P}{\partial t} + Pe u\left(r, \theta\right) \frac{\partial P}{\partial \xi} = \frac{\partial^2 P}{\partial \xi^2} + r\frac{\partial}{\partial r}\left(\frac{1}{r}\frac{\partial P}{\partial r}\right) + \frac{1}{r^2}\frac{\partial^2 P}{\partial \theta^2}. \tag{1.2}$$

The second-order derivative in the radial direction can be decomposed into one 'convective' term and one dissipative term as

$$r\frac{\partial}{\partial r}\left(\frac{1}{r}\frac{\partial P}{\partial r}\right) = \frac{1}{r}\frac{\partial P}{\partial r_1} + \frac{\partial^2 P}{\partial r^2}. \tag{1.3}$$

The radial convection term has a weak singularity at $r = 0$ and can be processed with an a priori step of random walk. By analogy with equation (1.1), the equivalent SDEs in the

† Email address for correspondence: gqchen@pku.edu.cn

cylindrical coordinates read

$$\left.\begin{aligned} \mathrm{d}\xi &= Peu\left(r,\theta\right)\mathrm{d}t + \sqrt{2}\mathrm{d}w_1 \\ \mathrm{d}r &= \tfrac{1}{r}\mathrm{d}t + \sqrt{2}\mathrm{d}w_2 \\ \mathrm{d}\theta &= \sqrt{2}\mathrm{d}w_3 \end{aligned}\right\}$$

When concerned with the axisymmetric mean concentration, the three-dimensional CDE may be averaged over θ and the equivalent SDEs reduce to the first two rows of (1.4). The rigorous proof of relations between SDEs and CDE under coordinate changes can be found in the book (see Section 4.8 of Chirikjian 2009, p. 130). In the present work, the total amount of particles is at least 100000 and the time step is less than 10^{-4} second for illustration in the main text and Supplementary Material. The Monte–Carlo simulation outweighs standard numerical techniques especially at short times for its absolute stability, simple manipulation and above all exact simulation of Dirac delta sources (Houseworth 1984; Guan *et al.* 2023).

2. Application to Couette flow in a channel

In this section, we present results for a channel Couette flow with the velocity profile $u(z)$ between two parallel plates, with ξ and z denoting the longitudinal and vertical coordinates, respectively. The system is governed by the dimensionless CDE in two dimensions

$$\frac{\partial C}{\partial t} + Peu(z)\frac{\partial C}{\partial \xi} = \frac{\partial^2 C}{\partial \xi^2} + \frac{\partial^2 C}{\partial z^2}, \tag{2.1}$$

under the conditions

$$\left.\begin{aligned} C|_{t=0} &= \delta(\xi)F\left(z\right), \\ \int_{-\infty}^{\infty}\mathrm{d}\xi\int_0^1\mathrm{d}zC &= 1, \\ C \to 0 \text{ as } |\xi| &\to \infty, \\ \left.\tfrac{\partial C}{\partial z}\right|_{z=0} = \left.\tfrac{\partial C}{\partial z}\right|_{z=1} &= 0, \end{aligned}\right\} \tag{2.2}$$

where $F\left(z\right)$ is the initial vertical distribution of the solute.

The spatial moment of concentration could be defined as

$$C_n(z,t) = \int_{-\infty}^{\infty}\xi^n C(\xi,z,t)\mathrm{d}\xi. \tag{2.3}$$

With the conditions of

$$\xi^n\frac{\partial^n C}{\partial \xi^n} \to 0 \text{ as } |\xi| \to \infty (n=0,1,2,\ldots), \tag{2.4}$$

Aris (1956) has demonstrated that C_n constitutes the solutions of the following problems

$$\left.\begin{aligned} \tfrac{\partial C_n}{\partial t} - \tfrac{\partial^2 C_n}{\partial z^2} &= n(n-1)C_{n-2} + nPeuC_{n-1}, \\ C_n|_{t=0} &= F\left(z\right), \\ \left.\tfrac{\partial C_n}{\partial z}\right|_{z=0} = \left.\tfrac{\partial C_n}{\partial z}\right|_{z=1} &= 0. \end{aligned}\right\} \tag{2.5}$$

As obtained by Barton (1983), the analytical solutions for these moments can be sequentially derived through the method of separation of variables in parallel flows where the associated eigenvalue problem possesses a discrete spectrum of eigenvalues. Employing the same techniques as outlined in the main text, a streamwise expansion for the concentration can be formulated as

$$C(\xi, z, t) = \frac{C_0}{\sqrt{2\pi\kappa_2}} \exp\left[-\frac{(\xi-\kappa_1)^2}{\kappa_2}\right]$$

$$\times\left[1+\frac{\kappa_3}{3!\,(\kappa_2)^{3/2}}He_3\left(\frac{\xi-\kappa_1}{\kappa_2^{1/2}}\right)+\frac{\kappa_4}{4!\kappa_2^2}He_4\left(\frac{\xi-\kappa_1}{\kappa_2^{1/2}}\right)+\ldots\right], \tag{2.6}$$

wherein κ_n is the cumulant of the n-th order and could be obtained directly through central moments, as calculated later in §4. The method can be extended to encompass three-dimensional cases with various initial distributions, significantly expanding the spectrum of physical problems that can be effectively addressed through the utilisation of this model. For brevity, we only apply the fourth-order solution of the streamwise dispersion model for the Couette flow in a two-dimensional channel herein.

Consistent with the case of the tube flow in the main text, we introduce a longitudinal coordinate $x' = \xi - Pe\bar{U}t$ at the speed of mean flow velocity $\bar{U} \equiv \int_0^1 u(z)dz$. For comparison with the classical theoretical results, a normalised set of $(\bar{C}Pe, x'/Pe)$ is adopted. The mean concentration from a line source obtained by the streamwise dispersion model within Couette flow is illustrated in figure 1, alongside numerical simulations conducted through a Monte-Carlo simulation. Figure 1(a) displays the concentration distribution at the initial stage for an area source, i.e. $F(z) = 1$, showcasing a distinctive saddle-shaped pattern. At short times, convection emerges as the dominant mechanism governing solute distribution. Solely accounting for convection yields a concentration distribution resembling a rectangle under uniform shear. However, when the influence of diffusion is factored in, owing to the presence of non-penetration boundary conditions, the soluble matter tends to accumulate in proximity to the wall, resulting in the formation of concentration peaks at both ends, as shown in figures 1(a)–(d). This phenomenon is also observed in circular tube flow, but in that context, the peak concentration is confined to the wall at $r = 1$, generating a skewed uni-modal concentration distribution. In the case of Couette flow, characterised by its anti-symmetrical velocity profile about $z = 0.5$, the mean concentration maintains this symmetry. As time elapses, the peaks at both ends gradually coalesce, ultimately giving rise to a normal distribution, as illustrated in figures 1(e) and (f).

3. Effects of Péclet numbers and initial conditions

Subsequently, we have performed supplementary computations to explore cases at a diminished Péclet number of $Pe = 100$, originating from an area source. As depicted in Figure 2, the analytical model demonstrates strong concordance with the numerical findings. In the case of soluble matter in a solvent flowing slowly through a tube, the impact of convection is promptly attenuated by molecular diffusion, facilitating a more rapid transition from skewed profiles to Gaussian distributions. Conversely, at a greater Péclet number, the disparity in spatio-temporal scales is so pronounced that capturing the comprehensive evolution of the concentration distribution becomes notably intricate (Guan *et al.* 2021, 2022).

Furthermore, our discussion has been extended to encompass initial sources at $r_0 = 0, 0.5$, and 1, and an area source with $Pe = 100$, as depicted in figure 3. For area and ring sources released at different radial positions during the intermediate regime, convection dominates along each streamline. When it comes to area and ring sources released at diverse radial positions during the intermediate regime, convection prevails along every streamline. Given

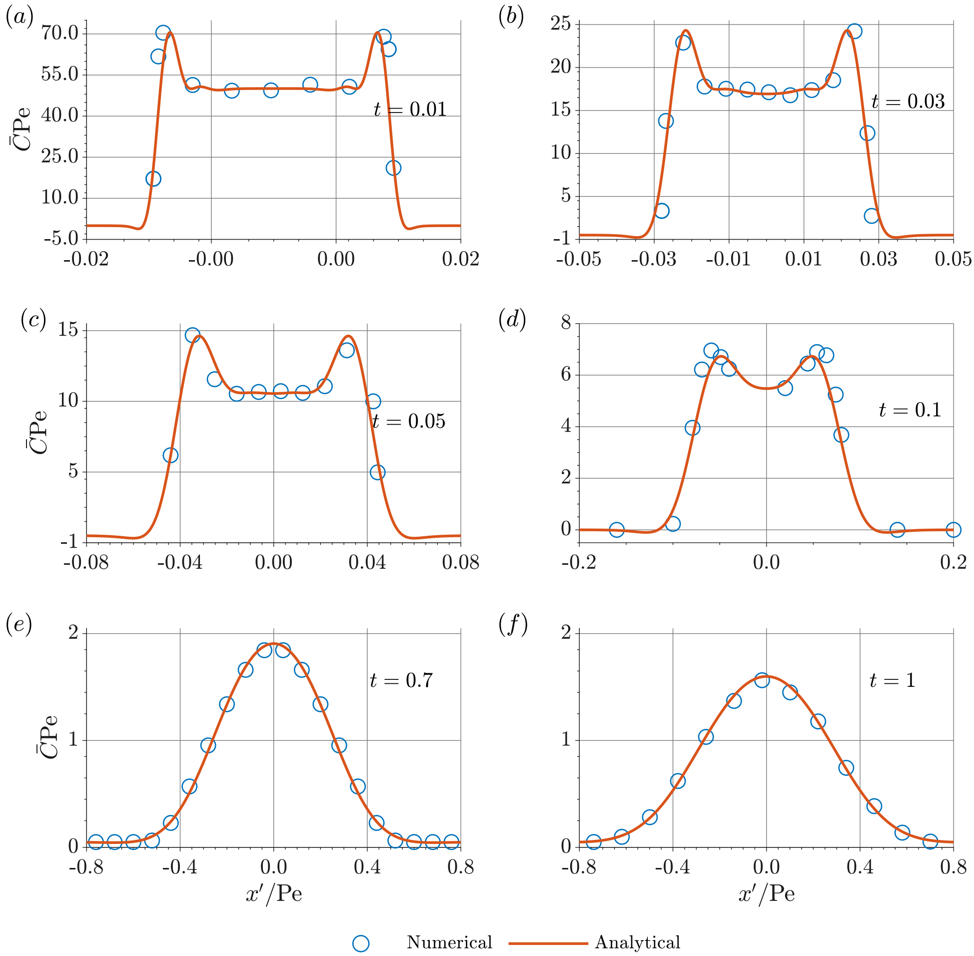

Figure 1: Mean concentration from a line source in a Couette flow.

the different convective velocity at each radial position, the soluble matter cloud is subject to distortion by shear, where the initial conditions dictate whether the peak of the mean concentration is convected downstream or remains near the wall at a slower pace. This, in turn, results in the depiction of right-skewed and left-skewed profiles, as illustrated in figures 3(a and b). Subsequently, the impact of transverse diffusion is more pronounced, causing the skewed profiles to become smoother and gradually transition into a Gaussian distribution, as illustrated in figures 3(c and d).

4. Correlation and generalisation of long-time asymptotic expansions

The spirit of the streamwise dispersion theory in local moment space can be applied to various long-time asymptotic expansions. We clarify the correlation of the present expansion with other long-time asymptotic expansions. Taylor (1953) first separated the scale of time and space, and experimentally proved the mean concentration can be governed only by longitudinal dispersion for long times in a moving x'-coordinate as

$$K_2 \frac{\partial^2 \bar{C}}{\partial x'^2} = \frac{\partial \bar{C}}{\partial t}, \tag{4.1}$$

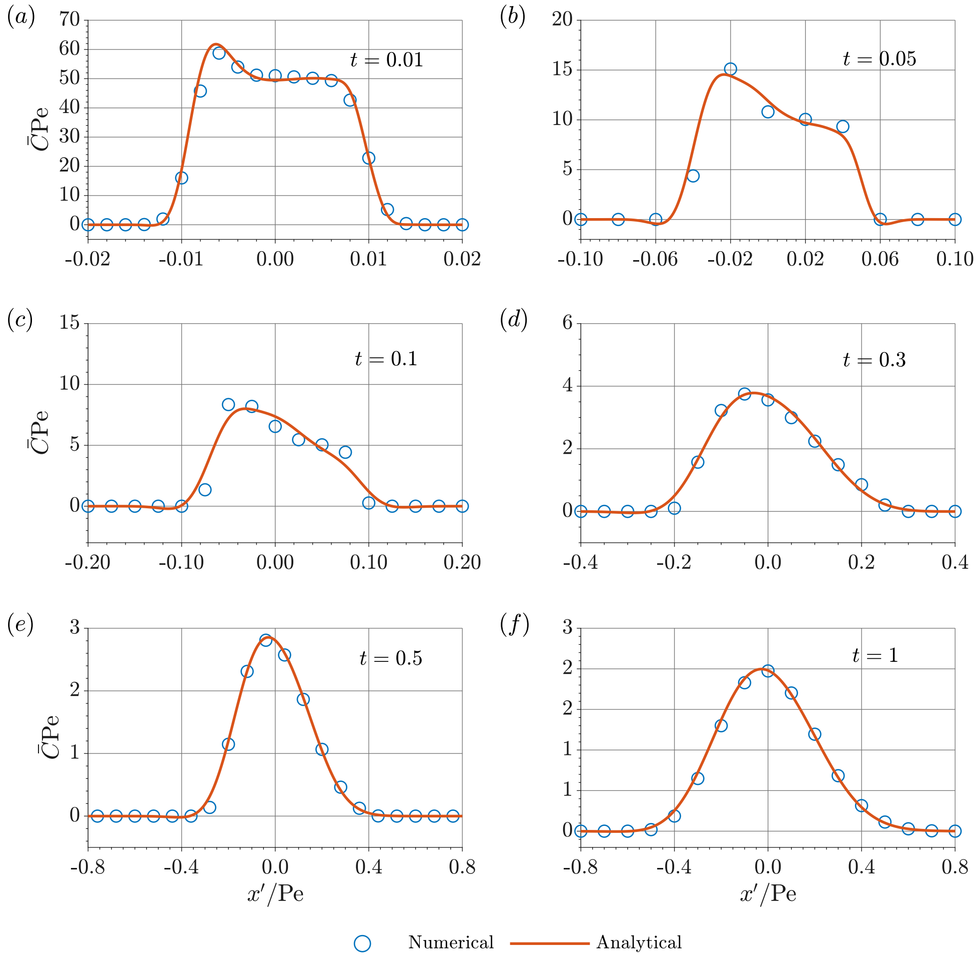

Figure 2: Mean concentration from an area source with Pe = 100 in a tube Poiseuille flow.

where K_2 is the second-order effective diffusivity in the consistent notation in the main text. Inspired by this simplified model, Taylor proposed in a moving coordinate system as

$$C = \bar{C} + \frac{U^* a^{*2}}{D^*} g^{(1)} \frac{\mathrm{d}\bar{C}}{\mathrm{d}x'} \tag{4.2}$$

and naturally introduced the second-order derivatives (Taylor 1954). By analogy with (4.2), Gill (1967) suggested that C can be expanded in an infinite series

$$C = \bar{C} + \sum_{n=1}^{\infty} f_n\left(t\right) \frac{\partial^n \bar{C}}{\partial x'^n}, \tag{4.3}$$

where f_n is the time-dependent coefficients of n-th order in Gill's model. The core of complete solution of Gill's model is the series expansion

$$C = \sum_{n=0}^{\infty} f_n \frac{\partial^n \bar{C}}{\partial x'^n}, \tag{4.4}$$

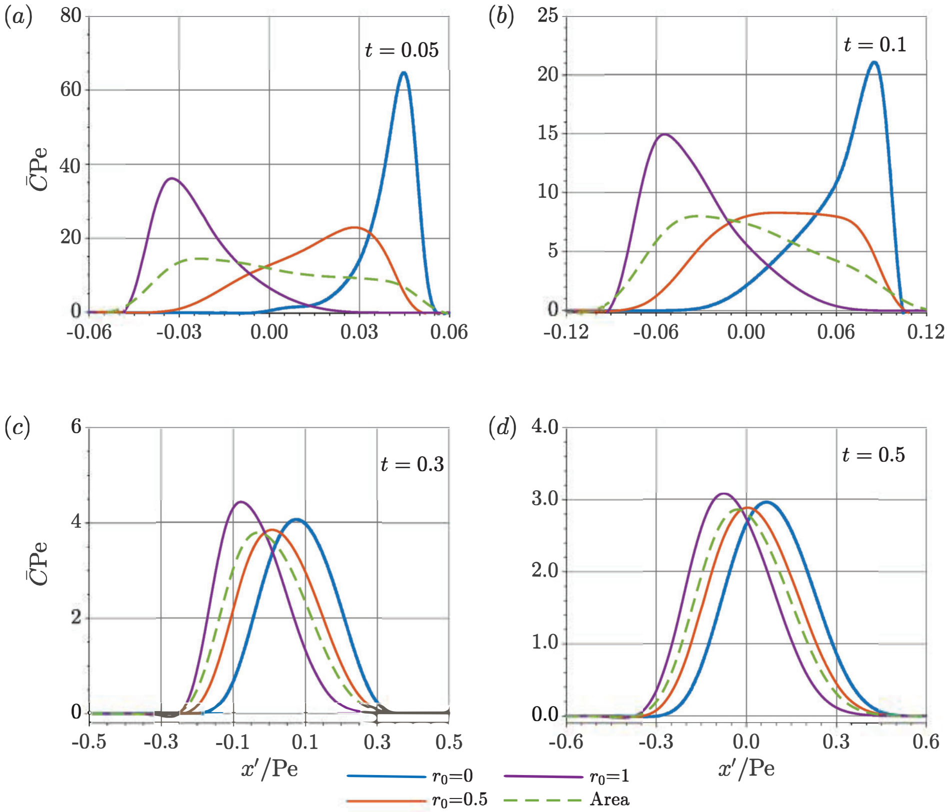

Figure 3: Axial distributions of mean concentration of a solute with different initial conditions for $Pe = 100$ in a tube Poiseuille flow. Sample times: (a) $t = 0.05$, (b) $t = 0.1$, (c) $t = 0.3$, (d) $t = 0.5$.

and another assumption

$$\frac{\partial \bar{C}}{\partial t} = \sum_{m=0}^{\infty} K_m \frac{\partial^m \bar{C}}{\partial x'^m} \tag{4.5}$$

proposed in the work of Gill (1967) can be deduced by substituting (4.3) into the governing equation of mean concentration. Jiang & Chen (2018) presented the Taylor–Gill solution up to the fourth order

$$\bar{C} = \mathcal{F}_{\bar{\omega}}^{-1}\left\{\exp\left[\sum_{n=0}^{3}(-\mathrm{i}x')^n\bar{\omega}_n + (-\mathrm{i}x)'^4\bar{\omega}_4\right]\right\} = \bar{C}_{(3)} * \left\{\frac{1}{\sqrt[4]{-\bar{\omega}_4}} W\left[\frac{x'}{\sqrt[4]{-\bar{\omega}_4}}\right]\right\} \tag{4.6}$$

Here $\bar{\omega}$ is denoted with an overbar to differentiate from the definition of time-dependent coefficient ω derived by spacial concentration moments. Correspondingly, $\bar{\omega}$ can be calculated with mean concentration moments. On the other hand, the change of averaged moments to spatial ones embodies the opinion of viewing from streamline perspective, viz.

$$\bar{C} = \int_0^1 2r\mathrm{d}r \int_{-\infty}^{\infty} \mathrm{d}\omega C_0 \exp\left[\sum_{n=1}^{\infty}\omega_n(t)(-\mathrm{i}\omega)^n\right] \mathrm{e}^{-\mathrm{i}\omega x'}. \tag{4.7}$$

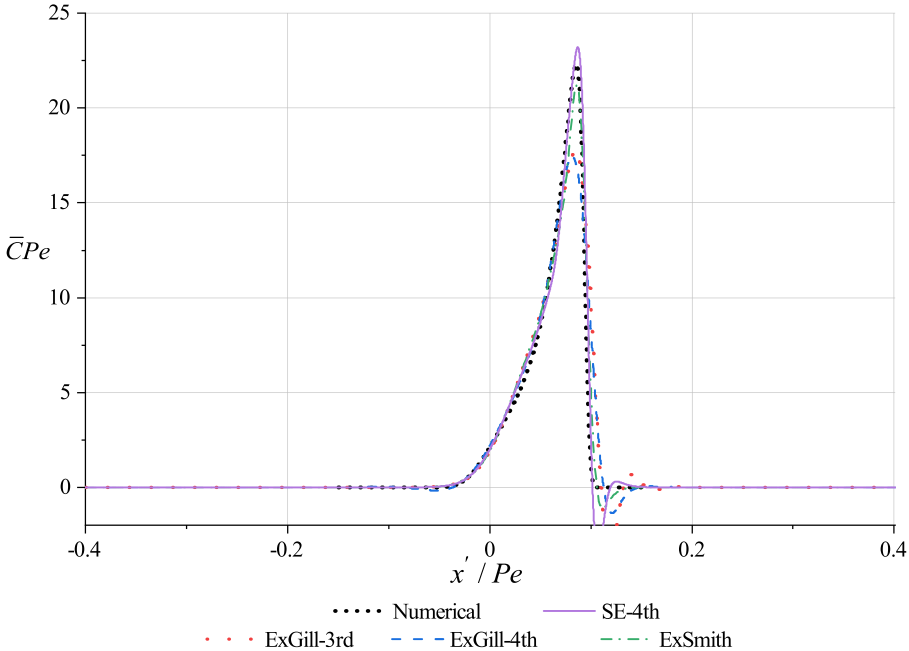

Figure 4: Comparisons of mean concentration $\bar{C}$ at $t = 0.1$ obtained by the present streamwise expansion (solid purple), third-order extended Gill's model (dotted red), fourth-order extended Gill's model (dashed blue), and third-order extended Gram–Charlie expansion of Smith (1982) (dash-dotted green) with the numerical results (coarsely dotted black). In all cases, $Pe = 10000$ and particles are discharged on the central axis initially.

This difference is significant as spatial concentration moments somewhat introduce a modified phase displacement during the transient period.

Another perspective is to view the concentration in the form of a Gaussian approximation. Chatwin (1970) assumed C could be expressed by the long-time expansions

$$C \sim \frac{C^{(0)}}{T} + \frac{C^{(1)}}{T^2} + \frac{C^{(2)}}{T^3} + \ldots, \tag{4.8}$$

wherein $C^{(p)}$ for each order p could be obtained successively, $T = M_C t^{1/2}$ and the constant M_C can be determined for algebraic convenience. It is remarked by Chatwin (1972) that the difference between C and $\bar{C}$ does not follow a Gaussian distribution. By substituting (4.8) into the advection–diffusion equation, and equating the coefficients to be zero, Chatwin eventually yields the long-time approximation

$$C \sim \bar{C} + \left(\frac{U^* a^2}{D^*}\right) g^{(1)} \frac{\partial \bar{C}}{\partial x'} + \left(\frac{U^* a^2}{D^*}\right)^2 g^{(2)} \frac{\partial^2 \bar{C}}{\partial x'^2} + \ldots. \tag{4.9}$$

This solution is similar to the Taylor-Gill model, though it only adapts to asymptotically long times so that the coefficients are independent of time. The undetermined coefficients can be calculated with the aid of concentration moment. Wu & Chen (2014) extended Mei's homogenization method to include an axial correction function accounting for the non-Gaussian effect at the initial stage. Their multi-scale perturbation method eventually results in

$$C = \bar{C} + F_1 \frac{\partial \bar{C}}{\partial x'} + F_2 \frac{\partial^2 \bar{C}}{\partial x'^2} + \ldots + F_n \frac{\partial^n \bar{C}}{\partial x'^n} + \ldots, \tag{4.10}$$

where F_n is the coefficient only as functions of spatial coordinates, equivalent to Chatwin's results. On the other hand, Chatwin's long-time expansion is slightly different from the normal perturbation method, since the small parameter (of the order of $t^{-1/2}$) has to be differentiated. Note that Chatwin's technique is indeed an Edgeworth form of Gram–Charlie Type A expansion at asymptotically long times (Chatwin 1970).

Since Chatwin (1970) has demonstrated an alternative approach regarding cross-sectionally averaged concentration in statistical theories, we could likewise extend Gill's dispersion model (Gill 1967) directly to the transverse concentration distribution. In this way tedious derivations for Gill's coupling equations of time-dependent coefficients are avoided. With the aid of moment generating function, we obtain

$$\begin{aligned} \tilde{C} &= \int_{-\infty}^{\infty} C e^{\mathrm{i}\omega x'} \mathrm{d}x' = \sum_{n=0}^{\infty} \frac{(\mathrm{i}\omega)^n}{n!} C_n \\ &= C_0 \left[1 + \mathrm{i}\omega \frac{C_1}{C_0} + \frac{(\mathrm{i}\omega)^2}{2} \frac{C_2}{C_0} + \cdots \right]. \end{aligned} \tag{4.11}$$

Applying the Fourier transform to Gill's transient dispersion model, yields

$$\frac{\partial \tilde{C}}{\partial t} = \sum_{n=0}^{\infty} f_n (-\mathrm{i}\omega)^2 \tilde{C}, \tag{4.12}$$

Given that the initial condition of concentration along x'-axis is in a special form of Dirac delta function, the initial condition of $\tilde{C}$ can be obtained

$$\tilde{C}\big|_{t=0} = (C_0)|_{t=0} \tag{4.13}$$

Thus the solution of $\tilde{C}$ reads

$$\tilde{C} = \exp\left[\sum_{n=0}^{\infty} \omega_n(t)(-\mathrm{i}\omega)^n \right] \tag{4.14}$$

where $\omega_n = \int_0^t \mathrm{K}_n(t')\,\mathrm{d}t'$, $K_n \equiv \overline{f_{n-2}/Pe^2 - u f_{n-1}} + 2\,(\partial f_n/\partial r)|_{r=1}$, and $f_{-1} = f_{-2} = 0$. Based on Taylor expansion of the exponential term in (4.14), $\tilde{C}$ can be expressed as

$$\tilde{C} = \mathrm{e}^{\omega_0} \left[1 + (-\mathrm{i}\omega)\omega_1 + \frac{1}{2}(-\mathrm{i}\omega)^2 \left(\omega_2 + \omega_1^2 \right) + \cdots \right] \tag{4.15}$$

Comparing (4.11) and (4.15) gives

$$\omega_0 = \ln C_0, \quad \omega_1 = -\tfrac{C_1}{C_0}, \quad \omega_2 = \tfrac{1}{2}\left(\tfrac{C_2}{C_0} - \tfrac{C_1^2}{C_0^2}\right), \quad \omega_3 = -\tfrac{1}{6}\left(\tfrac{C_3}{C_0} - 3\tfrac{C_1 C_2}{C_0^2} + 2\tfrac{C_1^3}{C_0^3}\right),$$

$$\omega_4 = \tfrac{1}{24}\left(\tfrac{C_4}{C_0} - \tfrac{3{C_2}^2 + 4C_1C_3}{C_0^2} + \tfrac{12C_1^2C_2}{C_0^3} - 6\tfrac{C_1^4}{C_0^4}\right), \cdots \tag{4.16}$$

That is, ω_n have been expressed with the aid of spatial concentration moments. With the inverse Fourier transform $\mathcal{F}_{\omega}^{-1}\left(\tilde{C}\right) = \frac{1}{2\pi}\int_{-\infty}^{+\infty}\tilde{C}e^{-\mathrm{i}\omega x'}\mathrm{d}\omega$, the solution of C' reads

$$C = \frac{C_0}{2\pi}\int_{-\infty}^{\infty}\exp\left[\sum_{n=1}^{\infty}\omega_n\left(t\right)\left(-\mathrm{i}\omega\right)^n\right]\mathrm{e}^{-\mathrm{i}\omega x'}\mathrm{d}\omega, \tag{4.17}$$

as an extended Gill's model from a streamwise perspective.

The solutions of mean concentration from the extended Gill's model of the p-th order is defined as $\bar{C}_{(p)}$. Analytical solutions of second and third order are respectively

$$\bar{C}_{(2)} = \int_0^1 \frac{C_0 Pe}{\sqrt{4\pi\omega_2}}\exp\left[-\frac{\left(x'+\omega_1\right)^2}{4\omega_2}\right]2r\mathrm{d}r, \tag{4.18}$$

and

$$\bar{C}_{(3)} = \int_0^1 \frac{C_0 Pe}{\left|\sqrt[3]{-3\omega_3}\right|}\exp\left(-\frac{\omega_2}{3\omega_3}x' - \frac{\omega_1\omega_2}{3\omega_3} + \frac{2\omega_2^3}{27\omega_3^2}\right)\mathrm{Ai}\left(\frac{-x'-\omega_1+\frac{\omega_2^2}{3\omega_3}}{\sqrt[3]{3\omega_3}}\right)2r\mathrm{d}r \tag{4.19}$$

where the first kind of Airy function is $\mathrm{Ai}(x') = \frac{1}{2\pi}\int_{-\infty}^{\infty}e^{\mathrm{i}\left(\xi x'+\xi^3/3\right)}\mathrm{d}\xi$. The fourth-order solution is derived in the form of convolution

$$\begin{aligned}\bar{C}_{(4)} &= \int_0^1 \mathcal{F}_{\omega}^{-1}\left\{\exp\left[\sum_{n=0}^{3}\left(-\mathrm{i}x'\right)^n\omega_n + \left(-\mathrm{i}x'\right)^4\omega_4\right]\right\}2r\mathrm{d}r \\ &= \int_0^1 C_{(3)} * \left\{\frac{1}{\sqrt[4]{-\omega_4}}W\left[\frac{x'}{\sqrt[4]{-\omega_4}}\right]\right\}2r\mathrm{d}r\end{aligned} \tag{4.20}$$

where $W(x') \equiv \mathcal{F}_{\omega}^{-1}\left[\exp\left(-x'^4\right)\right] = \frac{1}{2\pi}\left[2\Gamma\left(\frac{5}{4}\right)_0F_2\left(;\frac{1}{2},\frac{3}{4};\frac{x'^4}{256}\right) - \frac{1}{4}x'^2\Gamma\left(\frac{3}{4}\right)_0F_2\left(;\frac{5}{4},\frac{3}{2};\frac{x'^4}{256}\right)\right]$ and ${}_0F_2(;b_1,b_2;x')$ is the special form of the generalised hypergeometric function.

Smith (1982) investigated the Gaussian approximation in terms of Gram–Charlie Type A series expansion, with short- and long-time asymptotic results obtained respectively. By using the Chebyshev–Hermite polynomials, an extended model of Smith is derived (Smith 1982; Wang & Chen 2017), as

$$\bar{C} = \int_0^1 \frac{C_0}{\sqrt{2\pi\mu_2}}\exp\left[-\frac{\left(\xi-\mu_1\right)^2}{2\mu_2}\right]\left[\sum_{n=0}^{\infty}\frac{a_n}{n!\mu_2^{n/2}}He_n\left(\frac{\xi-\mu_1}{\sqrt{\mu_2}}\right)\right]2r\mathrm{d}r, \tag{4.21}$$

where the central moments μ_1 and μ_2 are defined as

$$\mu_1 = \frac{C_1}{C_0}, \quad \mu_2 = \frac{C_2}{C_0} - \frac{C_1^2}{C_0^2}. \tag{4.22}$$

We emphasise the exact streamwise cumulant of the n-th order could be computed from corresponding dispersion coefficients, as

$$\kappa_1 = \mu_1, \kappa_2 = \mu_2, \kappa_n = \frac{1}{2}\left(-1\right)^n n!\left(\frac{K_n}{K_2}\right)\omega^{2-n} + O(\sigma^{-n}), \quad n \geqslant 3. \tag{4.23}$$

In summary, the present streamwise solutions includes the accurate description of moments up to the fourth order. These different expanding approaches for concentration distribution have been extended in the spirit of the streamwise dispersion theory and checked in comparison to numerical results at $t = 0.1$, as shown in figure 4. The adopted streamwise expansion of fourth order in this work outweighs the others for the current application of fundamental delta Dirac releases due to its accurate description of moments and superior astringency, showing the generality of the streamwise dispersion theory. Significant discrepancies have been produced due to the incorporation of streamwise corrections in contrast with existing dispersion models, especially during the transitional regime. This new streamwise perspective could advance our understanding of macro-transport processes of passive solutes and active suspensions.

REFERENCES

ARIS 1956 On the dispersion of a solute in a fluid flowing through a tube. *Proc. R. Soc. Lond. A* **235** (1200), 67–77.

BARTON, N. G. 1983 On the method of moments for solute dispersion. *J. Fluid Mech.* **126**, 205–218.

CHATWIN, P. C. 1970 The approach to normality of the concentration distribution of a solute in a solvent flowing along a straight pipe. *J. Fluid Mech.* **43** (2), 321–352.

CHATWIN, P. C. 1972 The cumulants of the distribution of concentration of a solute dispersing in solvent flowing through a tube. *J. Fluid Mech.* **51** (1), 63–67.

CHIRIKJIAN, GREGORY S. 2009 *Stochastic Models, Information Theory, and Lie Groups*, vol. 1. Boston: Birkhäuser Boston.

GILL, W. N. 1967 A note on the solution of transient dispersion problems. *Proc. R. Soc. A* **298** (1454), 335–339.

GUAN, MINGYANG, JIANG, WEIQUAN, WANG, BOHAN, ZENG, LI, LI, ZHI & CHEN, GUOQIAN 2023 Pre-asymptotic dispersion of active particles through a vertical pipe: The origin of hydrodynamic focusing. *J. Fluid Mech.* **962**, A14.

GUAN, MINGYANG, ZENG, L., JIANG, WEIQUAN, GUO, XINLEI, WANG, P., WU, Z., LI, Z. & CHEN, GUOQIAN 2022 Effects of wind on transient dispersion of active particles in a free-surface wetland flow. *Commun. Nonlinear Sci. Numer. Simulat.* **115**, 106766.

GUAN, MINGYANG, ZENG, L., LI, CHENFENG, GUO, XINLEI, WU, YIHENG & WANG, P. 2021 Transport model of active particles in a tidal wetland flow. *J. Hydrol.* **593**, 125812.

HOUSEWORTH, J. E. 1984 Shear dispersion and residence time for laminar flow in capillary tubes. *J. Fluid Mech.* **142**, 289–308.

JIANG, WEIQUAN & CHEN, GUOQIAN 2018 Solution of Gill's generalized dispersion model: Solute transport in Poiseuille flow with wall absorption. *Int. J. Heat Mass Transf.* **127**, 34–43.

SMITH, RONALD 1982 Gaussian approximation for contaminant dispersion. *Q. J. Mech. Appl. Math.* **35** (3), 345–366.

TAYLOR, GEOFFREY INGRAM 1953 Dispersion of soluble matter in solvent flowing slowly through a tube. *Proc. R. Soc. Lond. A* **219** (1137), 186–203.

TAYLOR, GEOFFREY INGRAM 1954 Conditions under which dispersion of a solute in a stream of solvent can be used to measure molecular diffusion. *Proc. R. Soc. A* **225** (1163), 473–477.

WANG, PING & CHEN, G. Q. 2017 Contaminant transport in wetland flows with bulk degradation and bed absorption. *J. Hydrol.* **552**, 674–683.

WU, ZI & CHEN, GUOQIAN 2014 Approach to transverse uniformity of concentration distribution of a solute in a solvent flowing along a straight pipe. *J. Fluid Mech.* **740**, 196–213.